3972–3987 *Nucleic Acids Research, 2011, Vol. 39, No. 9* *Published online 17 January 2011*
doi:10.1093/nar/gkq1299

Design of a peptide-based vector, PepFect6, for efficient delivery of siRNA in cell culture and systemically *in vivo*

Samir EL Andaloussi[1,2,3,*], Taavi Lehto[2], Imre Mäger[2], Katri Rosenthal-Aizman[1], Iulian I. Oprea[3,4], Oscar E. Simonson[3], Helena Sork[2], Kariem Ezzat[1], Dana M. Copolovici[2], Kaido Kurrikoff[2], Joana R. Viola[3], Eman M. Zaghloul[3], Rannar Sillard[1,5], Henrik J. Johansson[6], Fatouma Said Hassane[7], Peter Guterstam[1], Julia Suhorutšenko[2], Pedro M. D. Moreno[3], Nikita Oskolkov[2,5], Jonas Hälldin[8,9], Ulf Tedebark[10], Andres Metspalu[8,9,11], Bernard Lebleu[7], Janne Lehtiö[6], C. I. Edvard Smith[3,*] and Ülo Langel[1,2]

[1]Department of Neurochemistry, Stockholm University, 106 92 Stockholm, Sweden, [2]Institute of Technology, Tartu University, 504 11 Tartu, Estonia, [3]Department of Laboratory Medicine, Karolinska Institute, 141 86 Huddinge, Sweden, [4]Iuliu Hatieganu University of Medicine and Pharmacy, 400023 Cluj-Napoca, Romania, [5]CePep AB, 104 30 Stockholm, Sweden, [6]Department of Oncology and Pathology, Science for Life Laboratory, Stockholm and Karolinska Institute, 171 76 Stockholm, Sweden, [7]UMR 5235 CNRS, Université Montpellier 2, 340 95 Montpellier Cedex 5, France, [8]Tartu University, Institute of Molecular and Cell Biology, 510 10 Tartu, [9]The Estonian Genome Centre of University of Tartu, 504 10 Tartu, Estonia, [10]GE Healthcare Bio-Sciences, 751 84 Uppsala, Sweden and [11]The Estonian Biocentre, 510 10 Tartu, Estonia

Received September 29, 2010; Revised and Accepted December 3, 2010

ABSTRACT

While small interfering RNAs (siRNAs) have been rapidly appreciated to silence genes, efficient and non-toxic vectors for primary cells and for systemic *in vivo* delivery are lacking. Several siRNA-delivery vehicles, including cell-penetrating peptides (CPPs), have been developed but their utility is often restricted by entrapment following endocytosis. Hence, developing CPPs that promote endosomal escape is a prerequisite for successful siRNA implementation. We here present a novel CPP, PepFect 6 (PF6), comprising the previously reported stearyl-TP10 peptide, having pH titratable trifluoromethylquinoline moieties covalently incorporated to facilitate endosomal release. Stable PF6/siRNA nanoparticles enter entire cell populations and rapidly promote endosomal escape, resulting in robust RNAi responses in various cell types (including primary cells), with minimal associated transcriptomic or proteomic changes. Furthermore, PF6-mediated delivery is independent of cell confluence and, in most cases, not significantly hampered by serum proteins. Finally, these nanoparticles promote strong RNAi responses in different organs following systemic delivery in mice without any associated toxicity. Strikingly, similar knockdown in liver is achieved by PF6/siRNA nanoparticles and siRNA injected by hydrodynamic infusion, a golden standard technique for liver transfection. These results imply that the peptide, in addition to having utility for RNAi screens *in vitro*, displays therapeutic potential.

INTRODUCTION

Since the discovery of siRNAs, a key mediator of RNA interference (RNAi), an ever increasing number of publications has affirmed their utility in inducing gene silencing (1–4). Not only have siRNAs been exploited in target validation studies but the technology has also raised tremendous attention as a potential therapeutic platform (2).

*To whom correspondence should be addressed. Tel: +46 8 5858 3651; Fax: +46 8 5858 3650; Email: edvard.smith@ki.se
Correspondence may also be addressed to Samir EL Andaloussi. Tel: +46 8 5858 3652; Fax: +46 8 5858 3650; Email: samir.el-andaloussi@ki.se

Lately, large-scale RNAi screens have been extensively exploited for studying gene function and to identify new disease targets. However, while it is possible to design siRNA libraries to target entire genomes, the applicability of large high throughput screens in mammalian cells is limited due to problems in siRNA delivery, especially into primary- and suspension cells. The anionic nature and large size of siRNAs unfortunately imply that the cell membrane constitutes an impermeable barrier. Numerous delivery systems have therefore been developed to increase cellular internalization and tissue distribution of siRNAs (3,4). Unfortunately most transfection strategies fail to fulfill the criteria of an optimal delivery system, namely to: transfect entire cell populations independent of cell type and confluence, be active in the presence of serum proteins, display minimal toxicity, and work systemically *in vivo*. Thus, universal, robust, simple and effective *in vitro* delivery methods must be developed before harnessing the benefits from large-scale RNAi screens.

Cell-penetrating peptides (CPPs) have the earmarks of promising delivery vectors since they enter entire cell populations in a non-toxic fashion (5,6). These relatively short cationic peptides have been used in various settings for conveying different types of macromolecules. As a result of the synthetic origin of most CPPs, they can be designed to have predetermined structures, and as an additional implication of their synthetic nature, CPPs can easily be modified with different chemical entities. To further widen their applicability, CPPs can be recombinantly expressed together with specific proteins or be used in combination with other delivery systems. Taken together, this opens the door to a myriad of possibilities to rationally design peptide-based delivery vehicles.

There are several reports on successful siRNA delivery *in vivo* by using e.g. cholesterol-functionalized siRNAs, lipid-based nanoparticles etc., some of which are being evaluated in clinical trials (7). Nevertheless, all these formulations have their limitations, e.g. activation of toll-like receptors (TLRs), delivery is restricted almost exclusively to the liver, tissue toxicity, to name a few. CPPs could theoretically offer several advantages over other available vectors, however, only a handful of publications have reported on CPP-assisted siRNA delivery (8). Some successful attempts have been made to design structurally well-defined CPPs for siRNA delivery, both *in vitro* and *in vivo*. For instance, the MPG-8 peptide has been used *in vivo* for intratumoral (i.t.) injections and cholesterol-modified MPG-8 for systemic delivery (9). Also, CPP-functionalized multifunctional envelope-type nano device (MEND) formulations have been used for i.t. and *ex vivo* siRNA delivery (10,11). While these CPP-based delivery systems rely on interactions between siRNAs and CPPs to form nanoparticles, other strategies have been exploited as well. Dowdy and colleagues approached the siRNA delivery-associated problems from a different angle. They used a CPP recombinantly expressed as a fusion protein with a double-stranded RNA binding domain (named Tat-DRBD), thereby masking the anionic nature of siRNAs (12). Although this system efficiently transfected siRNAs into primary cells in a non-toxic manner, transfection media devoid of negative glycosaminoglycans (GAGs) was generally required. Possibly for this reason, no systemic *in vivo* delivery data has yet been reported for this system (13). Albeit promising attempts for siRNA delivery have been made, there is still plenty of room for improvements in rational design of CPP-based vectors.

In light of the above, we set out to design a CPP-based siRNA-delivery system that could be robustly synthesized, easy to use and endowed with the desired delivery properties. Due to the negative charge of siRNAs and the cationic nature of CPPs, it is very cumbersome to generate covalent conjugates. However, it has been previously reported that CPPs with certain properties can be non-covalently complexed with siRNAs and be used *in vitro* (9,14) or, for targeted delivery, *in vivo* (15,16). Although this approach has worked in some laboratories, most CPPs fail to deliver siRNAs using this strategy (6,17). The likely explanation is that the complexes are retained intracellularly, inside endosomes following endocytosis (8). We hypothesized that by covalently introducing a potent proton-accepting moiety, i.e. a novel chloroquine analog (18) into a CPP (i.e. TP10), it would be possible to facilitate escape from acidic endosomal compartments by osmotic swelling and by delaying the acidification of the endosomes and, thereby, delaying the lysosomal degradation pathway. Furthermore, based on prior experience that stearylation improves the activity of TP10 in serum (19), a stearyl moiety was introduced, generating the PepFect 6 (PF6) peptide. TP10 was chosen in this study since it has been previously used successfully both *in vitro* and *in vivo* (20) for nucleic acid delivery. Furthermore, introduction of the above-mentioned chemical modifications in any other tested CPP had negligible effects on siRNA-delivery (data not shown).

The rationally designed PF6 peptide promoted significant siRNA-mediated RNAi responses *in vitro*, even in various refractory cells, and, perhaps most importantly, it facilitated significant siRNA-mediated gene knockdown in several tissues following systemic administration in mice. It should be stressed that these effects were achieved by using a single-component delivery system, without exploiting targeting ligands and without requiring PEGylation of the PF6/siRNA nanoparticles. Judging by these properties, the PF6 technology could overcome several limitations of many currently used siRNA delivery systems.

MATERIALS AND METHODS

Synthesis of the trifluoromethylquinoline derivative

4-Chloro-7-(trifluoromethyl) quinoline (3.8 g, 16.4 mmol) and *N*-methyl-2,2′-diaminodiethylamine (25 ml, 194.1 mmol) was heated (80°C, 2.5 h; 130°C, 3 h; 140°C, 2.5 h). After cooling to RT, cold DCM was added, the precipitate was filtered off and discarded. The organic phase was washed (5% $NaHCO_3$ aq × 2, H_2O × 2) and dried [$MgSO_{4(s)}$], and the solvent was removed under reduced pressure giving the *N*-(2-aminoethyl)-*N*-methyl-*N*′-[7-(trifluoromethyl)-quinolin-4-yl]ethane-1,2-diamine (QN) (4.5 g, 14.4 mmol, 83%, calculated mass: 312.3 Da,

found: 312.1 Da (Perkin-Elmer prOTOF™ 2000 O-TOF MALDI instrument). Crude product (>90% purity according to HPLC) was used without further purification.

TP10 synthesis

This was performed on a SYRO multiple peptide synthesizer (MultiSynTech GmbH) using a polystyrene-based Rink amide resin (0.4–0.6 mmol/g). Standard[7] Fmoc (9 H-fluoren-9-ylmethoxycarbonyl)-AA-OH [except Lys[7], Fmoc-Lys(Mtt)-OH] were coupled using HBTU (3 eq., *O*-benzotriazole-*N*, *N*, *N*′, *N*′-tetramethyl-uronium-hexafluorophosphate) as activating reagent and DIEA (6 eq., diisopropylethyl amine) as base.

Synthesis of PF6

Resin-bound TP10 [Fmoc-AGYLLGK(ε-Mtt)INLKA LAALAKKIL- Rink amide resin] was manually treated to generate the N-terminal free amine (35% piperidine, 40 min) followed by coupling of stearic acid, BOP [benzotriazol-1-yloxytris(dimethylamino)-phosphonium hexafluorophosphate] and DIEA in DCM for 1 h. To the ε-amino group of Lys[7] (deprotected by repeated washes of 1% TFA, 3–4% TIS in DCM 1–1.5 h), Fmoc-Lys(Fmoc)-OH (3–5 eq.) was coupled as HOAt (1-hydroxy-7-azabenzotriazole) ester. After Fmoc removal (35% piperidine, 40 min), repeated coupling and final Fmoc removal resulted in a lysine tree containing four free amino groups. These were treated with succinic anhydride (1.5 eq.) and DIEA (3 eq.) in DMF (dimethyl formamide) for 10 min. QN (2.5 eq. in DMF) was coupled over night to the succinic acid modified lysine tree [TBTU/HOBt (3 eq.) and DIEA (6 eq.)]. After cleavage [water/TIS/TFA 2.5/2.5/95 (v/v)], filtration, precipitation (cold ether) and drying (lyophilization), crude PF6 was obtained. PF6 was purified by RP-HPLC, C_{18} preparative column (5 μm), 45% acetonitrile (ACN)–water [0.1% TFA], 5 min; 45–85% ACN, 60 min and eluted at 80% ACN. After freeze-drying, purity was >90–95% (HPLC). Product was analyzed [alpha-cyano-4-hydroxy-cinnamic acid (α-CHCA) as crystallization matrix] by MALDI MS (Perkin-Elmer prOTOF™ 2000 O-TOF, positive mode); calculated mass: 4408.8 Da, found: 4410.4 Da. PF6 will be available for other scientists for RNAi response validation if requested.

Synthesis of siRNAs

All siRNAs, synthesized and purified at GE Healthcare, Uppsala, were stored at 500 μM at −20°C. Sequences of siRNAs: EGFP sense 5′-GGCUACGUCCAGGAGCGC ACC and as 5′-UGCGCUCCUGGACGUAGCCUU, Luciferase sense 5′-ACGCCAAAAACAUAAAGAAAG and as 5′-UUCUUUAUGUUUUUGGCGUCU, HPRT1 sense 5′-GCCAGACUUUGUUGGAUUUGAAATT and as 5′-AAUUUCAAAUCCAACAAAGUCUGGCUU, Oct4 sense 5′-ACUCGAACCACAUCCUUCUU and as 5′-GAAGGAUGUGGUUCGAGUUU.

Cell culture conditions

Cells were grown at 37°C, 5% CO_2 in humidified environment. HEK293, HeLa, U2OS, N2a, SH-SY5Y, Hepa1c1c7, HepG2, U87, RD4 and primary MEF cells were grown in 10% FBS-DMEM with glutamax. Bhk21 cells were grown in 10% FBS-GMEM with glutamax supplemented with 0.3% tryptose phosphate broth (Sigma). THP1, B16, Jurkat and K562 cells were grown in 10% FBS-RPMI-1640 media. All cells were supplemented with 0.1 mM non-essential amino acids (NEAA), 1.0 mM sodium pyruvate and antibiotics (100 U/ml penicillin and 100 mg/ml streptomycin). These chemicals were purchased from (Invitrogen, Sweden). HUVECs were grown on gelatinized cell culture plates in Endothelial Cell Growth Medium 2 supplemented with SupplementMix C39216 (PromoCell). C17.2 cells were grown in 10% FCS-DMEM High Glucose (4.5 g/l) with L-glutamine, 5% horse serum and 20 μg/ml gentamycin. mES cells were grown in DMEM high glucose (4.5 g/l) with L-glutamine, 0.1 mM NNEA, 1.0 mM sodium pyruvate, 15% ES-cell tested FBS, antibiotics, 0.1 mM 2-mercaptoethanol and 1000 U/ml leukemia inhibitory factor, using mitomycin C inactivated mouse embryonic fibroblasts as feeder monolayer. Luciferase stable cells were generated by lipofection of pGL3 luciferase plasmid (Clontech) under selection with Hygromycin (Sigma). Luc-HepG2 cells were generated by lentiviral transduction. EGFP-CHO cells were provided by Andres Merits.

Formulation, characterization and treatment with PF6/siRNA

PF6 (100 μM stock solution) was mixed with siRNA (10 μM stock solution) in MQ water in one-tenth of final treatment volume (i.e. 50 μl), using MR30 in serum free media or MR40 in serum experiments. Complexes were formed for 30 min at RT and added to cells, grown to 60% confluence in 24-well plate, in 450 μl growth media. After 4 h, 1 ml of fresh media was added to wells and cells were incubated for indicated times. Treatments with LF2000 and RNAiMAX were conducted in accordance with recommendations from manufacturer (Invitrogen), using 1 μl/well for 50 nM siRNA in 24-well plates. Transductin™ was used according to guidelines (IDT Technologies), using 6–7 μM reagent with 100 nM siRNA but performing experiments in serum supplemented or serum free media (instead of Q-serum devoid of GAGs). In luciferase experiments, cells were lysed using 100 μl of 0.1% Triton X-100 in Hepes Krebbs Ringer buffer. After 30 min lysis on ice, luciferase expression was measured using Promega Luciferase Kit on 96-well Glomax luminometer (Promega). If using Cy5-labled siRNAs, lysates were first analyzed by fluorometry using a Spectra Max Gemini (Molecular Devices) prior to luciferase measurements. For *in vivo* treatment trials, PF6/siRNA particles (MR30) were formed in MQ-water in half of the injection volume (i.e. 100 μl), using 2 mM PF6 and 0.5 mM siRNA stock solutions. After 30 min incubation, 100 μl of 10% glucose or 10.8% mannitol solution was added to the particles. Two hundred micro liter solution was injected into the tail-vein of mice.

Hydrodynamic infusions in tail vein of mice were carried out using 1 mg/kg siRNA in 2 ml saline buffer injected with high pressure. Hydrodynamic mean diameter of PF6/siRNA particles was determined (using a refractive index of 1.338) by DLS studies (Zetasizer Nano ZS apparatus, Malvern Instruments) and z-potential was measured using the same instrument.

Liposome leakage assay

Large unilamellar vesicles (LUV) were prepared by mixing dioleoylphosphatidylcholine (DOPC)/ dioleoyl-phosphatidylethanolamine (DOPE)/phosphatidylinositol (PI)/bis (monooleoylglycero) phosphate (LBPA) (Avanti polar lipids) (DOPC/DOPE/PI/LBPA: 5/2/1/2) and 10 μmol of the mixture in organic solvent (chloroform/ethanol: 9/1) was dried by evaporation under nitrogen atmosphere and rehydrated using 1 ml of 20 mM MES buffer containing 12.5 mM ANTS fluorochrome (8-aminonaphthalene-1,3,6-trisulfonic acid), disodium salt (Invitrogen), 45 mM DPX quencher (*p*-xylene-bispyridinium bromide) (Invitrogen) and 75 mM NaCl, pH 5.5. The lipid suspension was agitated on a vortex and submitted to five cycles of freeze/thawing before passage 21 times through 100 nm polycarbonate filter (Nucleopore, Whatman) using a mini extruder (Avanti polar lipids). Free dye and quencher were removed by gel filtration on a Sephadex G-50 column (Amersham Biosciences). Liposomes were eluted with 20 mM MES buffer, 145 mM NaCl, pH 5.5 and analyzed on a submicron particle size analyzer (Coulter N4, Beckman). Phosphatidylcholine was quantified using a LabAssay phospholipids kit (Wako) according to manufacturer's instructions. Liposomal leakage was measured on a luminescence spectrometer (Perkin Elmer LS 55) at pH 5.5 or 7.4.

Flow cytometry analysis and fluorescence microscopy

For FACS analysis, 6×10^4 cells/well were seeded onto 24-well plates one day before experiment. After treatment, cells were washed with PBS, trypsinized, resuspended in ice-cold PBS containing 2% FBS and analyzed on a BD LSRII flow cytometer (BD Biosciences) using FacsDiva software (BD Biosciences). For microscopy, 2×10^4 cells/well were seeded into Lab-Tek^{TM} 8-chambered cover glasses (Nunc; Thermo Fisher Scientific) 24 h before experiment. After treatment cells were washed with PBS, stained with trypan blue and imaged on Nikon Eclipse TE2000-U inverted microscope.

Immunocytochemistry

mES cells grown on gelatinized cover slips placed in 24-well plates using inactivated MEFs as feeder monolayer were transfected as described above. After 72 h, cells were fixed with 4% paraformaldehyde in PBS (15 min), permeabilized (2×15 min) with 0.25% Triton X-100 solution in PBS (PBST) and blocked with 5% normal goat serum (NGS). Cells were treated with 0.8 μg/ml rabbit polyclonal primary antibody to Oct4 (ABCAM) in solution of 2% NGS, in PBST for 1 h at RT, and washed 3×10 min with PBST. Secondary goat antirabbit Alexa-568 (2 μg/ml) antibody (Invitrogen) in solution of 2% NGS in PBST was incubated for 1 h at RT, and cells were washed 2×10 min with PBST supplemented with 0.5 μg/ml DAPI to stain the nuclei. Coverslips were mounted on glass slides using 30% glycerol in PBS. Cells were imaged using Nikon Eclipse TE2000-U inverted microscope.

RNA extraction and qPCR analysis

RNA from cultured cells and tissue samples was extracted using NucleoSpin RNA II Purification Kit (Macherey and Nagel) or TRIzol Reagent (Invitrogen), respectively. cDNA was synthesized with First Strand cDNA Synthesis Kit (Fermentas), HPRT1 mRNA expression was detected using $5 \times$ HOT FIREPol® EvaGreen® qPCR Mix Plus (ROX) (Solis BioDyne) on 7900HT Real-Time PCR System (Applied Biosystems). HPRT1 mRNA expression was normalized against internal standard GAPDH.

Cell viability assay

Ten thousand cells/well were seeded in 96-well plates and treated with 100 nM siRNA together with transfection reagents as indicated. The Wst-1 assay was used to assess metabolic activity after 24 h according to manufacturer's protocol (Roche) using a Tecan spectrophotometer.

Microarray analysis

RNA was amplified and biotinylated using the Illumina® TotalPrep RNA Amplification Kit (Ambion, Applied Biosystems) and purified, fragmented and hybridized to Illumina Human-6 V2 & V3 BeadChip arrays (Illumina). Background subtraction, expression summary, normalization, log base 2 transformation and MA-plots were carried out using R (Bioconductor).

Mass spectrometry-based proteomics analysis

Cell lysates were treated with DTT/iodoacetamide and trypsinized overnight. Samples were labeled with iTRAQ 8plex (Applied Biosystems) and separated by immobilized pH gradient—isoelectric focusing (IPG-IEF) on a narrow range strip (GE Healthcare) (21). Extracted fractions from the IPG-IEF were separated using a nano-LC system (Agilent1200) coupled to LTQ Orbitrap Velos MS (Thermo Scientific). Proteome discoverer 1.1 with Mascot 2.2 (Matrix Science) was used for protein identification searching IPI database (3.64), limited to a false discovery rate of $<1\%$ and ≥ 2 peptides/protein.

IL-1β, TNF-α and IL-6 analysis

THP1 cells were differentiated using phorbol myristate acetate (PMA) (10 ng/ml) for 48 h before experiment and seeded onto 24-well plate (2×10^5 cells/well). Cells were treated as previously. LPS (15 μg/ml) was used as positive control. Culture supernatants were collected at 4 and 24 h after treatment, and assayed for IL-1β and TNF-α by ELISA according to manufacturer's protocol (R & D systems). IL-6 and TNF-α levels in blood were analyzed at 24 h post i.v. injection of NMRI female mice

with 1 mg/kg PF6/siRNA, siRNA only, vehicle only (5% glucose) or LPS (10 μg). Blood was collected retro-orbitally and serum was purified using serum separation tubes (BD Bioscience). Serum (100 μl) was assayed using ELISA Max Deluxe Set (Biolegend) and absorbance measured on Spectra Max (Molecular Devices).

RNAi experiments *in vivo*

In HPRT1 experiments, C57Bl/6JOlaHsd (Harlan) females were utilized for treatments. Animals were randomized into four groups ($n = 3$–6) and treated as indicated. At 24 or 72 h, mice were sacrificed by cervical dislocation and tissues collected and rapidly frozen in liquid nitrogen (except for blood that was collected into heparinized tubes and stored at 4°C). Blood sample analysis of white blood cell count and levels of s-CRP was conducted by the United Laboratories at Tartu University Hospital. Clinical chemistry parameters (ALT/AST and creatinine levels) on serum from NMRI female mice, prepared as previously described, were analyzed after 72 h treatments by the Clinical chemistry laboratory at Karolinska University Hospital using IFCC standardized techniques. Lung, liver and kidney were dissected after 72 h and fixed in formalin, embedded in paraffin and stained with hematoxylin. Histology sections were analyzed by the Pathology department at Karolinska University Hospital. In luciferase experiments, NMRI adult female mice were injected with a dose of 10 μg UbCeGFPLuc plasmid using hydrodynamic technique (ref.). After 3 weeks, D-luciferin (150 mg/kg) was injected intraperitoneally and following 4 min incubation, bioluminescence imaging was performed in a Xenogen IVIS100 imager (Xenogen) using 5 min exposure and high-sensitivity setting. Mice were imaged in a ventral presentation to monitor liver-expression and quantified by total flux using Living Image Software (Xenogen). Animals were then randomized into four groups ($n = 4$ in each group) and treated as indicated and assayed at Day 3, 5, etc. During experiment, animals were anesthetized using 4% isoflurane. Experiments were approved by the Swedish local board for laboratory animals.

Statistical analysis

Results are presented as mean ± SEM. Statistical significance ($*P < 0.05$, $**P < 0.01$ and $***P < 0.001$) was calculated using one-way ANOVA with Tukey multiple comparison test.

RESULTS

Design of PF6

We aimed to develop a peptide-based carrier for siRNA delivery by introducing modifications into the well-characterized TP10 peptide (Figure 1a, compound 1). Successful carrier development necessitates solving two often occurring issues: (i) because the RNAi machinery resides in the cytoplasm of cells, it must be ensured that CPP/siRNA complexes, which are taken up by cells via endocytic pathways, are as promptly as possible released into the cytoplasm; and (ii) the CPP/siRNA complexes must be protected from being degraded in serum.

It is known that co-addition of the lysosomotropic agent chloroquine (CQ) in solution enhances endosomal release of peptide-based delivery vehicles. Therefore it was reasonable to assume that TP10, containing covalently attached CQ analogs (Figure 1a, compound 2), would more efficiently deliver siRNA into the cytoplasm and would also allow fine tuning of the overall *in vitro* concentration of these proton accepting moieties by changing the number of covalently attached CQ analogs. In contrast to CQ added in solution, a covalently attached CQ analog would exhibit an effective concentration only locally inside the endosomes. Also, we have previously shown that both the delivery efficiency and stability of TP10 are enhanced when the peptide is N-terminally stearylated (19) [Figure 1a, compound 3, PepFect 3 (PF3)]. Hence we hypothesized that TP10, containing both the fatty acid modification and a CQ analog, would have the required properties for siRNA delivery.

As previously reported (18), exchanging the quinoline-substituted 7-chlorine to a lipophilic trifluoromethyl group resulted in a significant increase in endosomolytic activity of the CQ analog. However, the number of carbon atoms between the two amines in the side-chain of the CQ analogs was of less importance. Furthermore, increasing the number of amines in the side chain from two to four gave only a slight increase in activity. Based on these data, we monoarylated one of the primary amines in *N*-methyl-2,2′-diaminoethylamine with 4-chloro-7-(trifluoromethyl)quinoline, which gave a suitable derivative (QN) that could be further attached to TP10 via a dicarboxylic acid linker, i.e. succinic acid. As previously reported (20) the side chain of Lys^7 residue of TP10 was found to be the preferred site for modifications. First, one succinylated QN was attached to the side-chain of Lys^7 (Figure 1a, compound 4), which resulted in slightly increased activity of the TP10 peptide (data not shown). We then hypothesized that by introducing several QN molecules, the effect would increase further. Incorporation of a lysine tree to the Lys^7 residue of TP10, followed by succinylation and covalent attachment of four QN molecules to the lysine tree, gave rise to the PF5 peptide (Figure 1a, compound 5). PF5 indeed promoted efficient siRNA-mediated RNAi responses in cell culture but, unfortunately, these effects were severely reduced in the presence of serum proteins (data not shown). Since we have previously shown that the delivery efficiency and stability of TP10 is enhanced when the peptide is N-terminally stearylated, we introduced both the QN and fatty acid modifications in order to increase the performance of the siRNA delivery vehicle in complete cell growth media, generating the PF6 peptide (Figure 1a, compound 6).

Characterization and evaluation of the endosomolytic design of PF6

To assess whether PF6 can form nanoparticles with siRNA, the peptide was co-incubated with siRNA in water at different molar ratios (MRs) ranging from 0–40 of peptide over siRNA and the size of particles was

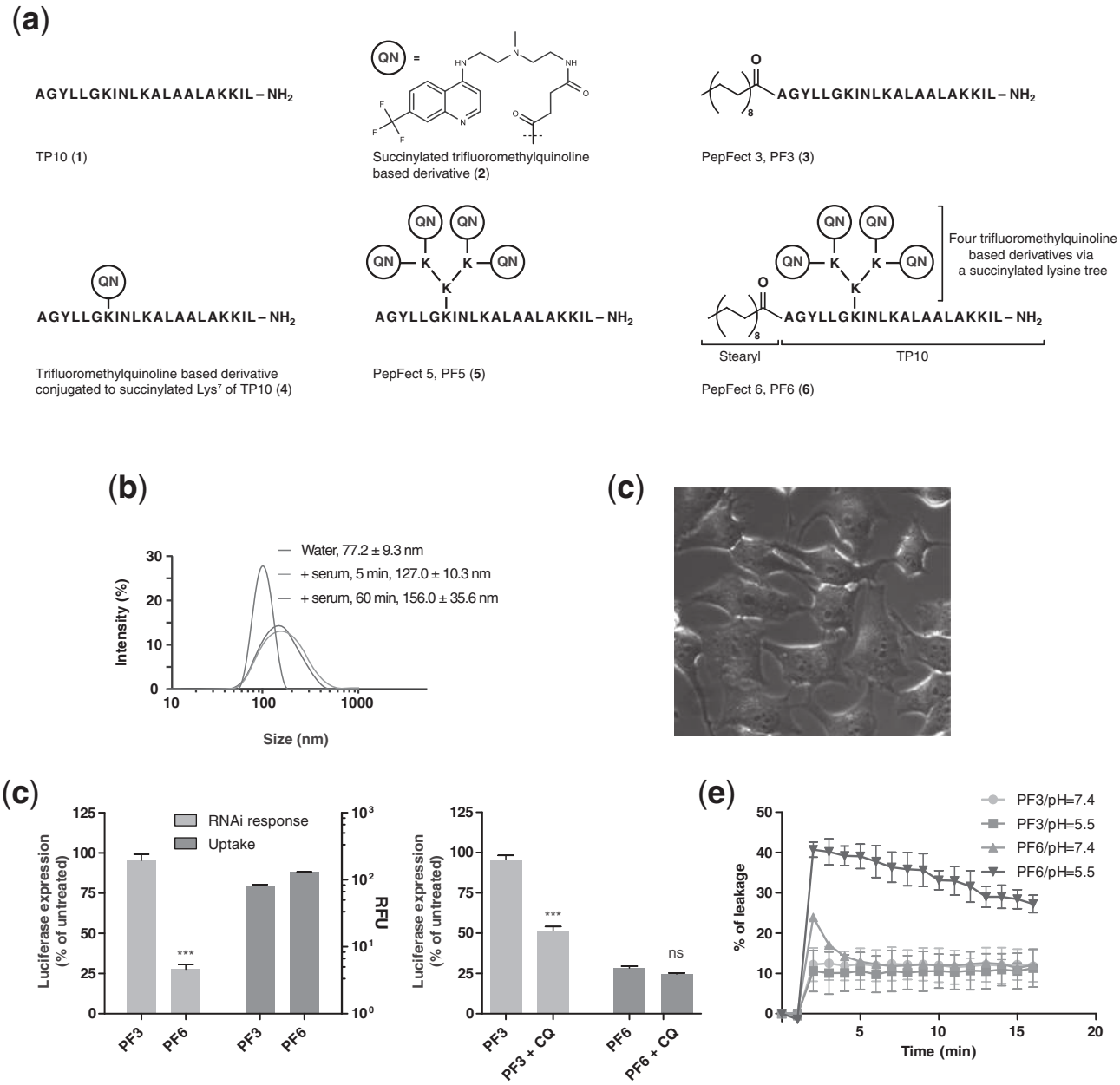

Figure 1. Rational iterative design and general properties of PF6. (**a**) Chemical structure of the different chemical intermediates of PF6: TP10 backbone (compound 1), succinylated trifluoroquinoline based derivative (compound 2), PepFect3 (compound 3), trifluoroquinoline based derivative conjugated to succinylated Lys7 of TP10 (compound 4), PepFect5 (compound 5) and PepFect6 (compound 6). (**b**) A representative DLS profile on the distribution of PF6/siRNA particles 30 min after formulation in water and at indicated time points after dilution in 10% serum in optiMEM. (**c**) Fluorescence microscopy overlay at 1 h after treatment of U2OS cells with 50 nM PF6/Cy5-siRNA. (**d**) Uptake (RFU) and RNAi response in luc-U2OS cells 24 h after treatment with 50 nM Cy5-labeled luc-siRNA complexed with PF6 or PF3 (left panel). RNAi response after same treatments with- or without co-addition of 100 μM chloroquine (right panel). (**e**) Liposome leakage at different pH after treatment with 50 nM PF3/siRNA or PF6/siRNA.

analyzed over time by dynamic light scattering (DLS). At all MRs, PF6 formed homogenous, unimodal nanoparticles with siRNA having particle sizes of 70–100 nm, which remained stable at 4°C for at least 4 weeks both in water with or without mannitol or glucose (Figure 1b and Supplementary Table S1). The presence of serum proteins generated a population of larger particles (125–200 nm) with wider distribution but, importantly, the population was intact for at least 1 h (Figure 1b). At all tested ratios in serum media, PF6/siRNA particles displayed a slightly negative surface charge, with zeta-potentials ranging from −7 to −11 mV.

To validate the endosomolytic properties of PF6, we initially assessed the potency of the peptide to promote endosomal escape of siRNA. As seen in Figure 1c, already after 1 h PF6/Cy5-labeled siRNA was endocytosed, judging by the extensive vesicular distribution. In order to estimate the degree of endosomal release conferred by the

proton-accepting QN moiety of PF6, it was compared to PF3, the identical peptide lacking the QN modification. Although both peptides promoted cellular uptake of Cy5-siRNA to the same extent, only PF6 induced siRNA-mediated gene silencing (Figure 1d, left panel). Furthermore, upon co-addition of CQ, PF3/siRNA-mediated RNAi was significantly increased while it had no impact on PF6/siRNA (Figure 1d, right panel). To corroborate these findings, a liposome leakage model was utilized in which peptide-imparted destabilization of liposomes at different pH can be assessed. As expected, PF6-induced liposome leakage was increased substantially when decreasing the pH, while PF3-mediated destabilization remained unaffected (Figure 1e). These results clearly illustrate the pH-dependent endosomolytic properties of PF6.

RNAi responses in reporter cells—PF6 versus lipofection

To date the majority of siRNA-transfections are carried out using cationic liposomes, such as Lipofectamine™ 2000 (LF2000). Thus, PF6 was compared to LF2000 in dose-response experiments using luciferase (luc)-stable human embryonal kidney (HEK) and human osteosarcoma (U2OS) cells. Not only did PF6 confer siRNA-mediated gene silencing dose-dependently, but more importantly, the response was relatively well-preserved in serum and significantly exceeded the activity of LF2000 (Figure 2a and Supplementary Figure S1a). At an siRNA concentration as low as 6 nM, significant RNAi responses were observed in both cell-lines and at higher siRNA concentrations, >90% gene silencing was obtained using PF6. The concentration of siRNA needed to knock down 50% of the target gene (i.e. IC_{50}) was ranging from 2.8 to 8.9 nM in commonly used adherent cell-lines including HEK, HeLa, U2OS, CHO, RD4, Hepa1c1c7 and Bhk21 cells (Supplementary Table S2). Importantly, the observed knockdown was siRNA-mediated and not imparted by the peptide, since 100 nM control siRNA formulated with PF6 (i.e. Ctrl) had no impact on gene expression. In keeping with previous studies, we rarely obtained >75% silencing using LF2000, even at 50 nM siRNA concentrations. By increasing the amount of liposomes, it was possible to obtain near 90% RNAi responses, however, this concomitantly resulted in severe cellular toxicity (data not shown). To fully validate the potential of PF6, another reagent, optimized for siRNA transfections, was included for comparison, namely Lipofectamine™ RNAiMAX (RNAiMAX). In the more refractory HepG2 hepatoma cell-line, we observed the same trend as in the other cell types, with PF6 being the most potent vector, and no significant differences were observed between LF2000 and RNAiMAX (Figure 2b and Supplementary Figure S1b).

Many transfection systems are strictly dependent on defined amounts of reagents in order to efficiently transfect cells. In order to address whether this applies also for PF6-mediated delivery, a dose-titration of PF6 was carried out and compared with both LF2000 and RNAiMAX. For PF6, we started at MR40 (i.e. the amount used in all other experiments in serum containing media) and titrated the concentration of PF6 down to MR10, keeping the siRNA amount constant. The same was done with the two lipid-based vectors. Interestingly, with PF6, as opposed to LF2000, the relative amount of peptide over siRNA could be varied, still leading to significant RNAi responses (Supplementary Figure S2a, left panel). Although essentially full silencing was observed using molar ratio 40 (MR40) and 50 nM siRNA, >80% silencing was observed using MR10 in different types of cells (Supplementary Figure S2a, right panel). Moreover, in contrast to both LF2000 and RNAiMAX, that are dependent on relatively low cell confluence for their performance, we observed only small variations in PF6/siRNA-mediated RNAi responses when varying cell densities (Figure 2c and Supplementary Figure S2b).

After quantitatively determining the magnitude of gene silencing, we addressed the percentage of cells undergoing RNAi by using CHO cells stably expressing EGFP, and monitoring expression after treatment with PF6/EGFP-siRNA complexes by flow cytometry and fluorescence microscopy. By treating cells with 50 nM PF6/siRNA in the presence of serum, entire cell populations underwent RNAi within 48 h, as judged by the complete shift in the FACS histograms as well as the lack of EGFP-positive cells under the microscope (Figure 2d and Supplementary Figure S2c). In contrast, a large fraction of the target population was not silenced by lipofection, using 100 nM siRNA. Another important aspect for successful implementation of RNAi is the persistence of gene silencing over time. After a single treatment with PF6/siRNA in EGFP-CHO cells, significant gene silencing was observed for 5 days with slower decay kinetics than with LF2000, using 50 nM siRNA (Figure 2e). Furthermore, repeating same treatments every third day gave a complete RNAi response for at least 8 days when using PF6/siRNA (Supplementary Figure S2d).

Endogenous gene knockdown using PF6/siRNA nanoparticles

After confirming the potency of PF6 in commonly used adherent cell-lines by reporter-gene silencing, we investigated the targeting of an endogenous gene, hypoxanthine phosphoribosyltransferase 1 (HPRT1), by measuring mRNA levels using qPCR. HPRT1 was chosen due to the long cellular half-life of the protein (~48 h) and thereby minimal impact on the vitality of the transfected cell and limited off-target effects of the specific HPRT1 siRNA sequence were expected (22). In order to accurately determine the degree of down-regulation, glyceraldehyde 3-phosphate dehydrogenase (GAPDH) was used as an internal standard for quantification. Initially, the kinetics of HPRT1 RNAi in human Hepa1c1c7 hepatoma cells was assessed. Strikingly, already after 4 h, >50% gene silencing was observed and the magnitude of RNAi increased over time with a 95% knock-down after 8 h with PF6, using 50 nM siRNA (Figure 3a). Silencing was much faster than with lipofection (Figure 3a), in keeping with the rapid endosomal release of siRNA when using PF6. Next, primary mouse embryonal fibroblasts (MEFs) were

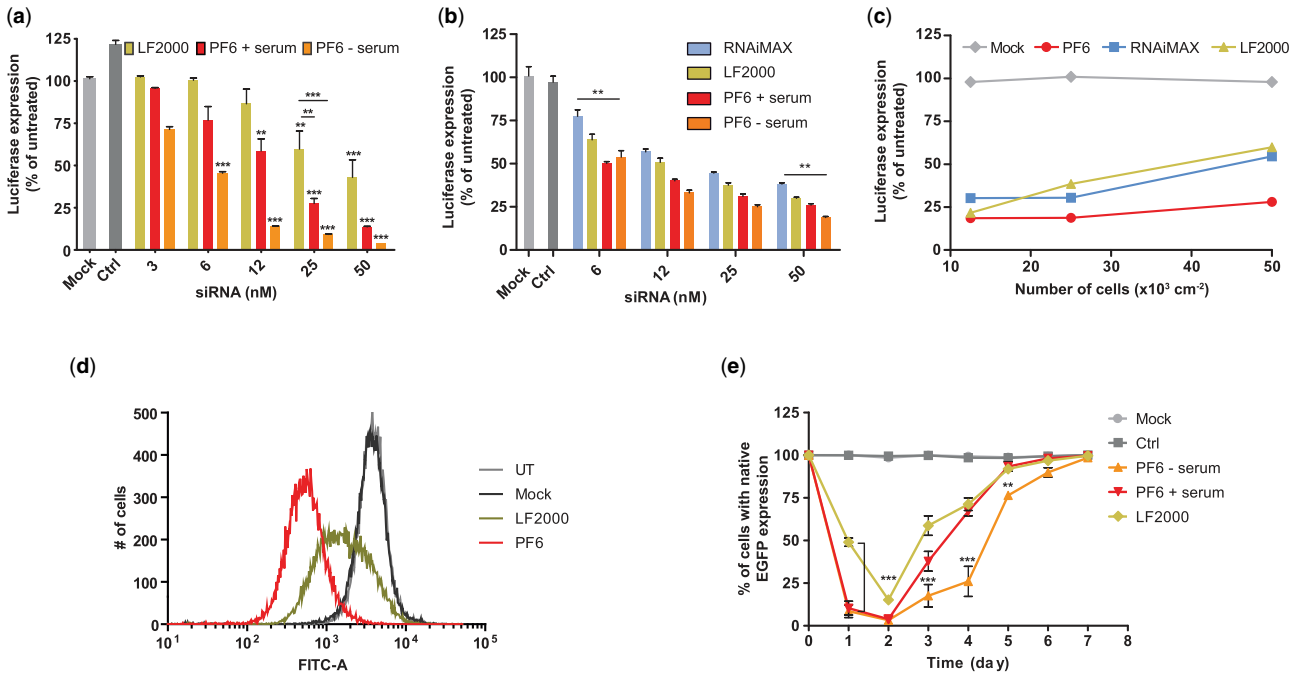

Figure 2. PF6-mediated siRNA delivery into reporter cells. (**a**) RNAi response in luc-HEK cells at 24 h after treatment with increasing concentration of luc-siRNA using PF6 or LF2000. One hundred nanomolar EGFP siRNA complexed with PF6 (ctrl) and 50 nM naked luc siRNA (Mock) was used as controls. Luminescence (RLU) was normalized to protein content and data presented as expression relative to untreated cells. (**b**) Dose-response in HepG2 cells after treatment as in (a). (**c**) Impact of cell confluence. Luc-U2OS cells seeded at indicated densities 1 day prior experiment were treated and analyzed as in (a) using 50 nM siRNA with PF6, LF2000 or RNAiMAX. (**d**) Flow cytometry histogram analysis of EGFP RNAi response in EGFP-CHO cells at 48 h post treatment with 100 nM free EGFP siRNA (mock) or complexed with LF2000 or PF6. (**e**) Flow cytometry analysis of EGFP knockdown decay kinetics following single treatment with siRNA. Treatments and subsequent analysis were performed as is in (d) but using 50 nM siRNA. Mock depicts only siRNA and Ctrl corresponds to 50 nM PF6/luc-siRNA. All experiments were performed at least three times in duplicate, showing the standard error of the mean (SEM).

used for screening of HPRT1 RNAi responses. Twenty-four hours after siRNA treatment, dose-dependent RNAi responses were observed using PF6 both in serum and serum free media, exceeding the activity of lipofection, with IC_{50} values of around 6 nM (Figure 3b).

Thereafter, human umbilical vein endothelial cells (Huvec) were assayed for RNAi. These cells are extremely difficult to transfect by chemical means, which limits their utility for large scale RNAi-screens. Since LF2000 was completely inactive in these cells, Transductin (i.e. Tat-DRBD) served as a positive control, in addition to RNAiMAX (Figure 3c). As expected, Transductin was efficient at transducing Huvec cells only when using high siRNA concentrations (100–400 nM) and when performing experiments under serum-free conditions. Using only 25 nM siRNA, we obtained stronger RNAi response with PF6 as compared to both Transductin and RNAiMAX at 100 nM siRNA (Figure 3c). Similar results were obtained in Jurkat T-lymphocyte cells. At 100 nM siRNA, transfections in serum- and GAG-free media were comparable between PF6 and transductin, but PF6 performed significantly better in serum-containing media (Figure 3d). A complete list of cells and targets used for RNAi experiments with corresponding IC_{50} values is found in Supplementary Table S2.

Finally, we investigated the possibility to target primary mouse embryonal stem (mES) cells using PF6, since these are very useful for modeling and understanding progression of disease but very difficult to transfect without inducing cellular differentiation. Freshly prepared mES-cells were subjected to siRNA treatment and a dose-dependent RNAi response was observed at 24 h after using PF6/siRNA particles, again exceeding the activity of the other reagents (Figure 3e). In order to confirm that cellular pluripotency was intact following PF6/siRNA treatment, expression of the pluripotency regulator Oct4 was assessed (23). Three days after treatment with PF6/HPRT1-siRNA, the expression level of Oct4 remained unaffected, with cells growing in sphere-like colonies, indicating that PF6 has negligible effects on cellular differentiation (Figure 4a). Accordingly, when using PF6/Oct4-siRNA we observed a significant reduction in Oct4 expression levels after 24 h (Figure 4b) and loss of colony growth within 72 h (Figure 4a), confirming that PF6 *per se* does not affect the pluripotency of cells.

In vitro toxicity of PF6/siRNA nanoparticles

Next, cell viability studies were performed, using the Wst-1 assay, in the most refractory cells. Although none of the reagents reduced viability of ES or Jurkat cells, the viability of Huvec cells was reduced substantially with all reagents except for PF6/siRNA (Supplementary Figure S3a–c). Furthermore, full-genome microarray analysis was carried out to exclude potential off-target transcriptome effects imparted by PF6. HeLa cells were transfected with either PF6/siRNA or LF2000/siRNA and

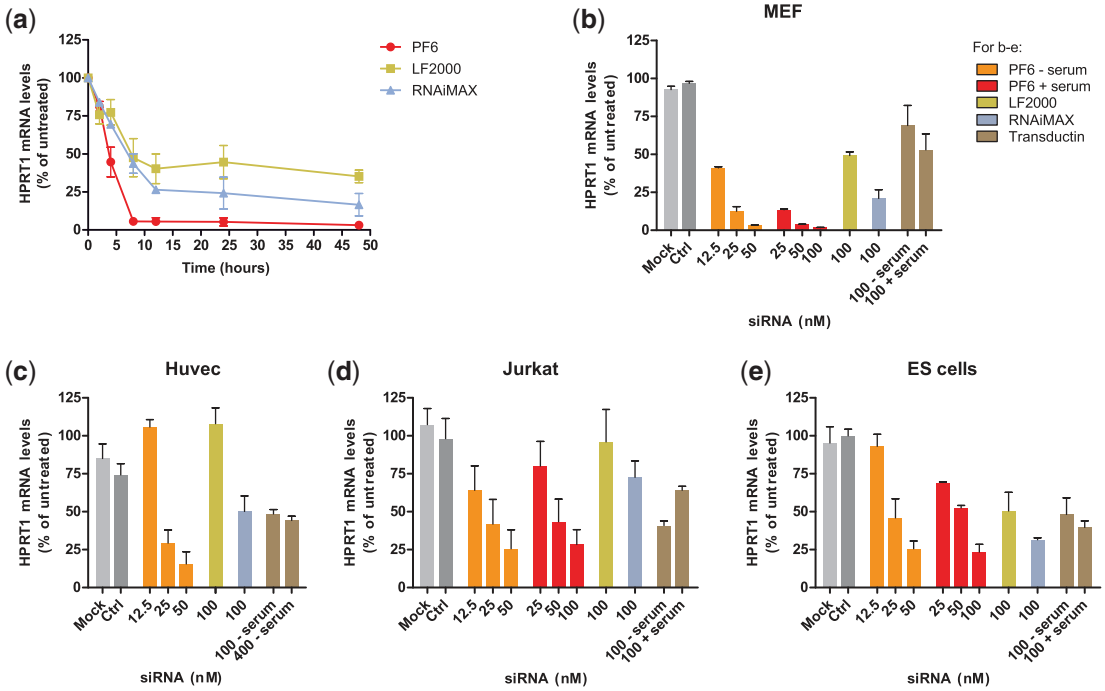

Figure 3. PF6-mediated siRNA delivery into refractory cells. (**a**) HPRT1 mRNA knockdown kinetics in Hepa1c1c7 cells following treatment with PF6, LF2000 or RNAiMAX in complex with 50 nM siRNA. Values represent mean normalized to GAPDH mRNA and presented as percent of untreated cells. qPCR analysis of HPRT1 mRNA levels at 24 h post treatment of (**b**) primary MEF cells, (**c**) Huvec cells, (**d**) Jurkat cells or (**e**) mES-cells with HPRT1-siRNA using PF6, LF2000, RNAiMAX or Transductin as indicated. One hundred nanomolar luc-siRNA complexed with PF6 (Ctrl) and 100 nM naked HPRT1-siRNA (mock) were used as controls. Key applies to b–e.

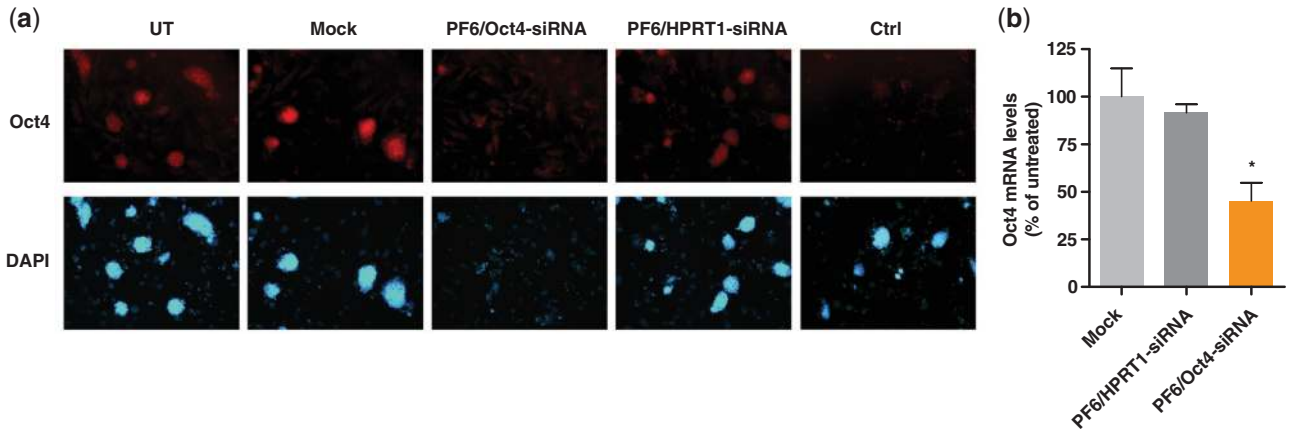

Figure 4. PF6/siRNA delivery into mES cells. (**a**) Fluorescence microscopy analysis of Oct4 expression and genomic staining (DAPI) in mES cells 72 h after treatment with PF6/HPRT1-siRNA, PF6/Oct4-siRNA and Oct4-siRNA only (mock). Ctrl depicts cells without primary antibody. (**b**) Oct4 RNAi response measured by qPCR 24 h after treatment with 50 nM PF6/Oct4-siRNA or PF6/HPRT1-siRNA. GAPDH was used as internal standard.

mRNA was analyzed at 24 h post treatment using a 1.6-fold increase/decrease filter to assess alterations. Noticeably, expression of more than 10 transcripts was significantly altered by LF2000 treatment whereas only one was affected by PF6 in addition to the HPRT1 target (Figure 5a). Naked siRNA had no significant impact on the transcriptome (data not shown). However, since overall mRNA and protein levels do not necessarily correlate (24), mass spectrometry-based proteomics was carried out. The expression of 18 proteins was significantly altered upon transfection with LF2000 compared to 12 proteins only in PF6 samples out of 2347 proteins identified (Figure 5b). Considering the scale of proteome coverage the number of deregulated proteins is very low. Similar results were obtained using a non-targeting EGFP-siRNA although the number of off-target proteins was significantly higher. Out of 4212 proteins identified and quantified, 140 proteins were de-regulated with PF6 and more than 300 with RNAiMAX, with several proteins overlapping (Figure 5c). These

discrepancies between the two siRNAs could be explained by the fact that HPRT1 siRNA has been optimized to reduce off-targeting in contrast to EGFP-siRNA.These results clearly show that PF6 displays lower cytotoxicity than commonly used lipid-based reagents.

Inflammation responses of PF6/siRNA *in vitro* and *in vivo*

After confirming the potency of PF6 in various cell cultures, we next sought to evaluate whether this compound could be applied for systemic delivery of siRNA in mice. An important parameter for *in vivo* delivery of siRNAs is to avoid triggering inflammatory responses (25). This was assessed in transformed human monocytic THP1 cells, where PF6 had negligible effects on the release of tumor necrosis factor (TNF)-α and interleukin (IL)-1β as compared to the positive control lipopolysaccharide (LPS) after 4 and 24 h treatments (Supplementary Figure S3d). These results were further corroborated *in vivo* where negligible induction of the inflammatory mediator IL-6 was observed 24 h after systemic administration of 1 mg/kg PF6/siRNA (Figure 6a). Also, TNF-α was not detected (data not shown) and the number of white blood cells as well as the level of C-reactive protein remained unchanged (Table 1), again indicating minimal inflammatory responses.

Systemic delivery of PF6/siRNA nanoparticles

The lack of inflammatory responses in combination with the efficient RNAi responses observed in cell culture encouraged us to further investigate the potential of PF6 for systemic delivery of siRNA. We chose to target HPRT1, since it is abundant in all tissues and the siRNA has been carefully optimized to minimize off-target effects. PF6 was formulated with HPRT1-siRNA or with control siRNA in water in half of the injection volume (i.e. 100 µl) at MR30. After 30 min, 100 µl of 10% mannitol solution was added to the complexes. HPRT1-siRNA was formulated with PF6 at doses ranging from 0.25 to 1 mg/kg siRNA and administered i.v. into mice. After 24 h, only modest gene silencing was observed in different organs at the highest dose (data not shown). Given that the highest silencing in cell cultures was observed at 48 h, additional treatments were carried out measuring HPRT1 silencing at 72 h using a 1 mg/kg dose. Whereas control treated animals displayed

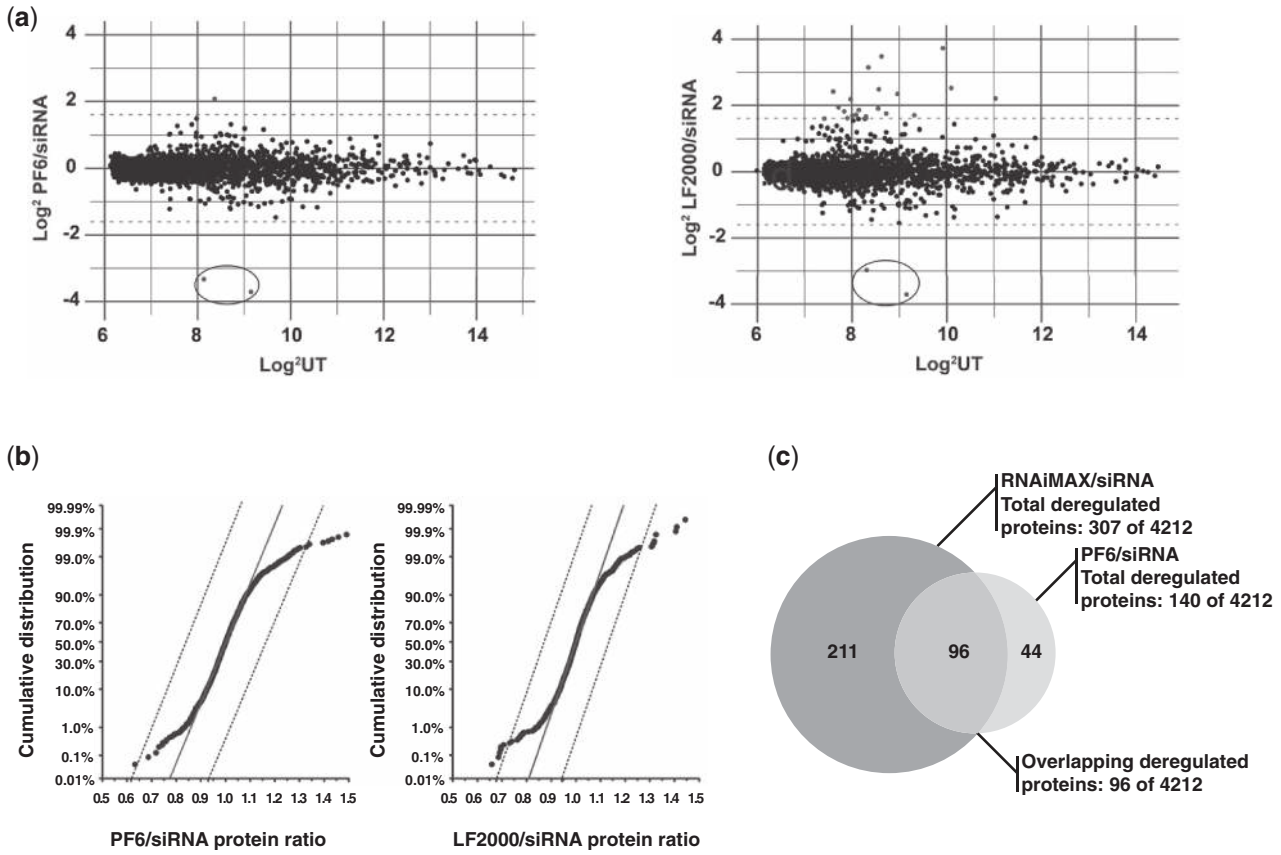

Figure 5. Analysis of the transcriptome and proteome after PF6/siRNA treatment. (**a**) Full-genome microarray analysis profile after 24 h of HeLa cells treated with PF6 or LF2000 complexed with 50 nM HPRT1-siRNA. Red line indicates a 1.6-fold increase/decrease and blue and red dots indicate genes with significantly altered expression compared to untreated cells. (**b**) Mass-spectrometry based proteomic analysis of HeLa cells after treatment with 100 nM siRNA in serum-supplemented media either using PF6 or LF2000. Results were normalized to treatments with only siRNA and presented as normal probability plot with a 99% confidence limit. (**c**) Mass-spectrometry based proteomic analysis of HeLa cells after treatment with 100 nM EGFP-siRNA in serum-supplemented media either using PF6 or RNAiMAX. Results were normalized to treatments with only siRNA and presented as Venn diagram displaying the deregulated proteins with each reagent.

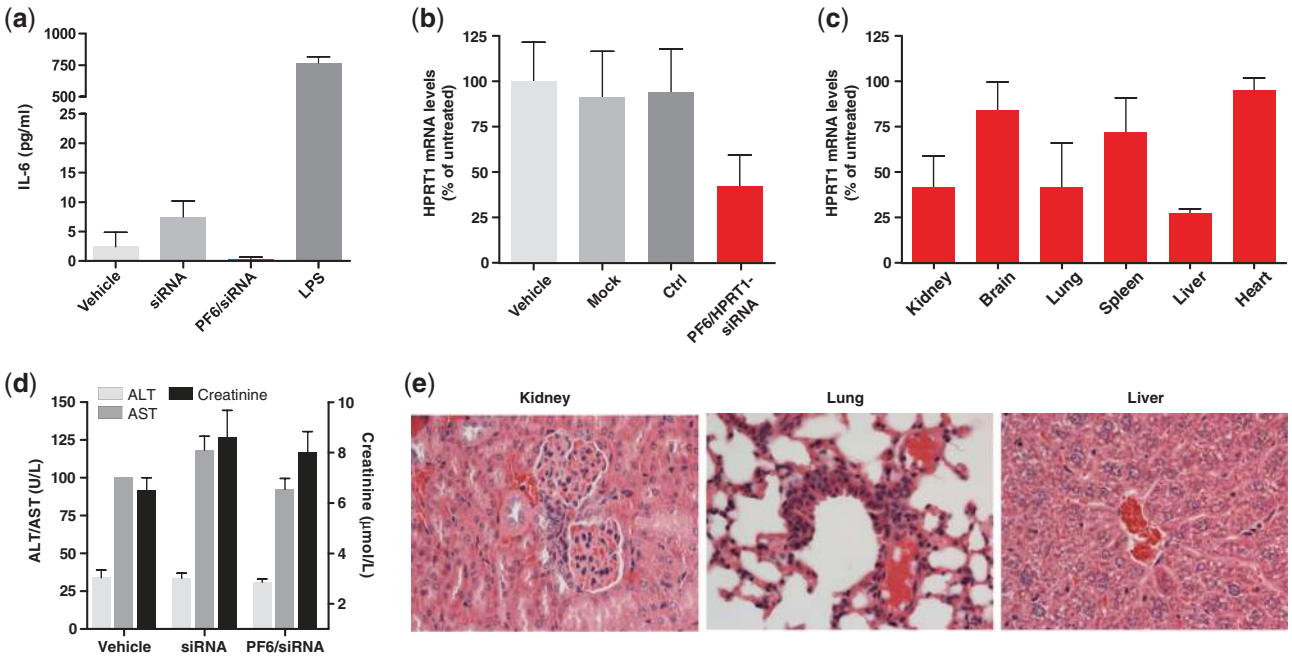

Figure 6. PF6-mediated siRNA delivery *in vivo*. (**a**) Analysis of IL-6 serum levels by ELISA 24 h following i.v. administration of 1 mg/kg of naked siRNA, PF6/siRNA formulated in 5% glucose or glucose only (vehicle). LPS (10 µg) was used as positive control ($n = 5$ for each group). (**b**) HPRT1 knockdown in kidney at 72 h post i.v. treatment with 1 mg/kg of PF6/HPRT1-siRNA. Vehicle (5.4% mannitol), naked siRNA (mock) and 1 mg/kg of PF6/luc-siRNA (Ctrl) were used as controls. Organs were lysed, mRNA extracted and HPRT1 mRNA measured by qPCR. These are mean values of HPRT1 normalized to GAPDH mRNA and presented as percent of untreated animals. Error bars indicate SEM, $n = 3$–6 for each group. (**c**) HPRT1 RNAi response in indicated organs 72 h after systemic delivery of 1 mg/kg PF6/HPRT1-siRNA formulated in 5.4% mannitol. Organs were lysed, mRNA extracted and HPRT1 mRNA measured by qPCR. These are mean values of HPRT1 normalized to GAPDH mRNA and presented as percent of untreated animals. Error bars indicate SEM, $n = 3$–6 for each group. (**d**) Transaminase (ALT/AST) and creatinine serum levels at 72 h after treatment as in (a) ($n = 5$ for each group) and corresponding histopathology analysis of hematoxylin–eosin stained tissue sections (kidney, lung and liver) from mice treated with 1 mg/kg PF6/siRNA (**e**). Except for (a), all *in vivo* formulations were administered in 5.4% mannitol solution.

Table 1. Clinical chemistry and hematology parameters for PF6/siRNA treated mice

Treatment group	Spleen weight (mg)	Creatinine (µmol/l)	ALT (U/l)	AST (U/l)	RBC ($\times 10^{12}$/l)	WBC ($\times 10^{9}$/l)	CRP (mg/l)
Vehicle	109.0 ± 8.0	6.5 ± 0.5	33.9 ± 5.1	100.4 ± 0.2	8.9 ± 0.4	5.0 ± 0.8	0.06 ± 0.01
siRNA	91.6 ± 5.2	8.6 ± 1.1	33.6 ± 3.3	118.3 ± 9.1	9.3 ± 0.3	4.7 ± 0.6	ND
PF6/siRNA	113.7 ± 9.8	8.0 ± 0.8	30.7 ± 2.1	92.3 ± 7.3	8.6 ± 0.5	4.3 ± 0.7	0.09 ± 0.02

ALT, alanine transaminases; AST, aspartate transaminases; RBC, red blood cells; WBC, white blood cells; CRP, C-reactive proteins.

no alterations in HPRT1 levels, PF6/siRNA-treated animals had significantly reduced expression of HPRT1 in kidneys (Figure 6b). RNAi responses were also observed in other tissues than kidney with the most prominent effects in liver and lungs (Figure 6c).

Importantly, these treatments were not associated with any acute toxicity according to the body weight loss calculations after 72 h (Supplementary Figure S3e). Although PF6/HPRT1 siRNA treatment reduced the body-weight, this is likely a result of HPRT1 knockdown, since PF6/luc-siRNA had no impact on the weight. Accordingly, liver transaminase levels (ALT/AST) remained at the levels of vehicle-treated mice 72 h post treatment with 1 mg/kg of PF6/luc-siRNA (Figure 6d), suggesting negligible effects on liver function. Similarly, serum creatinine levels were unaffected by the same treatment, thus confirming intact kidney function (Figure 6d). These results were supported by histopathological examinations of tissue sections where liver, kidney and lung histology appeared normal with no signs of acute toxicity (Figure 6e). A list of examined clinical chemistry and hematology parameters is given in Table 1.

To further validate the potency of PF6 *in vivo*, an additional mouse model was utilized. Mice expressing luciferase in the liver were treated with 0.2 or 1 mg/kg of PF6/luc-siRNA and assayed over 15 days by means of full body *in vivo* bioluminescence imaging (Figure 7 a and b). While naked luc-siRNA was unable to induce an RNAi response, PF6/siRNA-treated animals displayed reduced expression of luciferase for 2 weeks, reaching 75% silencing at day 5, when using the 1 mg/kg dose (Figure 7a). Even at a dose as low as 0.2 mg/kg, 50% gene silencing was observed when using PF6 (Figure 7b). Furthermore, i.v.-injected PF6/siRNA nanoparticles and naked siRNA administered via hydrodynamic injection produced the same RNAi effect, reducing luciferase

expression in the liver at comparable levels (Figure 7c). This is extremely encouraging, since hydrodynamic injection is considered one of the most efficient means of transducing liver (26). Collectively, the results illustrate the non-toxic nature and high potency of PF6 for systemic siRNA delivery.

DISCUSSION

Modulation of gene expression using RNAi technology has received immense attention in recent years. However, the anionic nature and large size of siRNAs unfortunately imply that the cell membrane constitutes an impermeable barrier that impedes harnessing the full potential of this technology. Thus, the key challenge in the RNAi field is to efficiently deliver siRNA molecules into the cytoplasm of cells. In the past we have had great success with one particular peptide, TP10, in the delivery of a wide array of cargoes, and we therefore iteratively modified this peptide to render it an efficient siRNA delivery vehicle. Our design aimed to solve two often occurring problems: (i) endosomal entrapment of material following endocytosis and (ii) the instability of CPPs in serum-containing environment. We hypothesized that incorporation of CQ analogues into CPP backbone would mimic the pH buffering and osmotic endosome swelling effects of CQ (27). Hence, we introduced four novel trifluoromethylquinoline-based derivatives (QN) via a succinylated lysine tree into the peptide sequence to improve endosomal release of siRNA and, secondly, a stearic acid moiety was attached to the N-terminus of TP10 to increase the serum stability of the peptide.

Different groups, including ourselves, have previously shown that CPPs can form particles with negatively charged ONs (including siRNAs) with a diameter of 100–300 nm (9,28).

Indeed, by simply mixing PF6 with siRNA in water, stable nanoparticles are formed within minutes which remain stable for weeks. This is a clear advantage compared to other efficient *in vivo* siRNA delivery systems that require complicated particle formation procedures (10,29,30). The mean diameter of PF6/siRNA nanoparticles, formed at various MRs, remains well below 200 nm similarly to other efficient siRNA nanoparticle formulations. In contrast to previous studies using MPG-peptide derivatives (9,28), we did not observe any particle aggregation at the higher MRs, instead, particles were slightly smaller in size and more homogenous. Moreover, particle size remained in this range also in the presence of serum, where water-formed

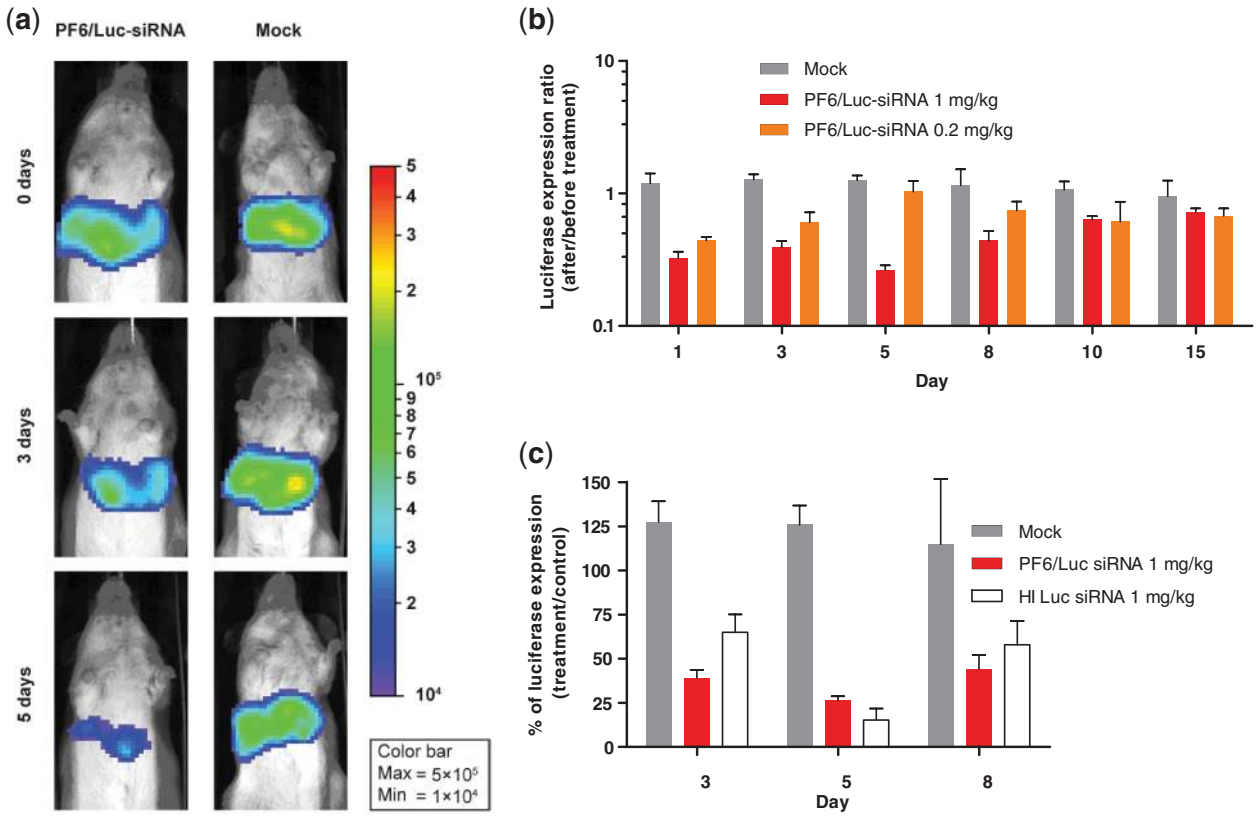

Figure 7. Assessment of PF6-mediated siRNA delivery *in vivo* using a bioluminescence model. (**a**) *In vivo* bioluminescence imaging of luciferase expression following i.v. delivery of 1 mg/kg of luc-siRNA, with or without PF6, at Day 3 and 5 post injection in animals with expression of luc from liver. (**b**) Luc knockdown over time after treatments with 0.2 or 1 mg/kg of PF6/luc-siRNA or 1 mg/kg naked luc-siRNA (mock). (**c**) Luc knockdown over time after treatments with 1 mg/kg luc-siRNA using hydrodynamic injection (HI) or 1 mg/kg of PF6/luc-siRNA. Naked luc-siRNA (mock) (1 mg/kg) was used as control. At least four animals were included in each treatment group. All *in vivo* formulations were administered in 5.4% mannitol solution.

particles often aggregate. Thus the particles should be suitably sized for *in vivo* conditions (9–11,31). To our knowledge, this is the first time the size of CPP/siRNA complexes have been analyzed by DLS in the presence of serum and these results suggest that PF6/siRNA particles are extremely stable. Interestingly, the PF6/siRNA nanoparticles are even more stabilized in mannitol and glucose, which are commonly utilized excipients for *in vivo* formulations.

After confirming the formation of stable, nano-sized particles, we next validated the endosomolytic design of the peptide. Although some CPPs (e.g. MPG derivatives) have been reported to work by direct translocation, most other CPPs in complex with cargo are evidently endocytosed (32). For example, we have previously shown that the endocytic pathway is determined by the chemical nature of the peptide. While purely cationic CPPs are macropinocytosed, amphipathic peptides, such as TP10, utilize classical clathrin-mediated endocytosis for internalization (33). Common for all studies showing endocytic uptake of CPPs is that co-addition of CQ drastically increases the biological activity of the delivered cargo, emphasizing that endosomal sequestration is a main limiting factor for most CPPs. In line with most other CPPs, when associated with cargo, we here confirm that PF6/siRNA nanoparticles are internalized via endocytosis, judged by the extensive vesicular distribution observed by fluorescence microscopy. To assess the endosomolytic properties of the QN-conjugated PF6, it was compared to PF3, which lacks the modification. Both peptides displayed similar uptake but only PF6 was able to promote siRNA-mediated RNAi. The greater ability of PF6 to promote endosomal escape was further supported by the fact that co-addition of free CQ in solution increased PF3/siRNA-mediated RNAi significantly while the same treatment had no impact on PF6-mediated siRNA delivery. This was confirmed in the liposomal leakage model where, at endosomal pH, PF6 had significantly higher destabilizing capacity of liposomes than PF3, and by the rapid PF6-mediated RNAi kinetics. These results clearly illustrate the pH-dependent endosomolytic properties of PF6, which enable fast release of siRNA into the cytoplasm.

The endosomolytic design rendered PF6 highly efficient in promoting siRNA-mediated RNAi in various cells, targeting either reporter genes (EGFP and luciferase) or endogenous genes (HPRT1 and Oct-4). In contrast to lipofection, PF6 promoted siRNA-mediated gene silencing in entire cell populations and, thus, dose-dependently exceeded the activity of the commercial lipofection reagents in practically all tested cells. Most importantly, the activity was well preserved in serum. Furthermore, while primary cells and suspension cells remain relatively refractory to most transfection strategies, PF6 efficiently promoted siRNA-mediated, dose-dependent gene silencing in different refractory cells such as Huvec, Jurkat, C17.2 neuronal stem cells and ES-cells with IC_{50} values ranging from 10 to 50 nM. These results collectively show that PF6 has the potential to transfect different cell types without affecting the phenotype of cells, which opens new possibilities for large-scale RNAi screens in disease-relevant primary cells. Furthermore, many siRNA transfection systems, such as lipofection, are strictly dependent on defined amounts of reagents and certain cell densities to be efficient. Thus, small variations in lipid amount or cell confluence might drastically affect their performance. In contrast, the exact molar ratio between siRNA and PF6 as well as the cell density could be varied, retaining the RNAi effect. These are clear advantages when PF6 is compared to other peptide- and cationic lipid-based vectors (9,10) because this allows optimizing transfection conditions when working with sensitive cell-lines. Also, being insensitive to varying cell confluence is very important for *in vitro* screens that require different end-points, and for successful *in vivo* implementation, where the target is intact tissues.

It is well-established that high transfection levels are commonly associated with significant cellular toxicity. For example, lipofection typically displays a linear correlation between efficiency and toxicity. At the recommended dosing, both LF2000 and RNAiMAX display only minor, non-significant, cytotoxicity but the achieved siRNA-mediated knockdown is unfortunately not complete. By increasing the lipid amount in siRNA experiments, RNAi responses of 85% can be achieved in regular adherent cells but the viability of cells concomitantly decreases drastically. Therefore, when screening for novel siRNA-delivery vectors it is pivotal to both analyze knockdown levels and to account for potential long-term toxicity. A major reason for the increased interest in CPPs in recent years is that they are considered to be relatively non-toxic for cells. However, it has been previously reported that CPP-related toxicities can occur at high peptide concentrations, especially when using amphipathic peptides such as TP10 (34,35). Thus, we investigated the potential toxicity of PF6. As judged by the Wst-1 assay as well as microarray and proteomics data, PF6 delivers siRNA to its target cells in a non-toxic manner.

After confirming the potency of PF6 in cell culture, we next assessed the suitability of the vector for systemic delivery of siRNA in mice. Using the HPRT1 housekeeping gene as a target, we observed pronounced knockdown in liver, kidney and lung, following systemic delivery of PF6/HPRT1-siRNA, possibly reflecting their high blood supply. The majority of previous other successful RNAi reports are indeed based on results achieved from the liver, whereas efficient gene knockdown in other organs requires much more complicated strategies and multicomponent delivery vectors (29,30). Strikingly, we observed >60% gene silencing also in kidneys and lung, by using PF6 as a single-component vehicle without additional targeting motifs. To corroborate the applicability of PF6 for *in vivo* delivery we could exclude most of the general toxic and immunogenic side-effects. Obviously, an important parameter for *in vivo* delivery of siRNAs is to avoid triggering inflammatory responses (25). Naked siRNAs are known to frequently stimulate inflammatory responses (36–39). Thus, an optimal vector should shield the siRNA through the endo-lysosomal pathways, where most TLRs are located and concurrently

not be immunogenic *per se*. PF6 effectively shielded the delivered siRNA from TLRs, suggested by the negligible immunogenic response, both *in vitro* and *in vivo*. Histopathological examination did not show any signs of toxicity in liver, lung or kidneys, and several other tested clinical or hematological parameters remained unaffected. This contrasts to many other polycationic vectors that have been exploited *in vivo* where, in particular, kidney and lung toxicity has been reported (40,41).

Based on the encouraging results of strong RNAi response in liver we utilized another animal model to analyze gene silencing in liver only. In this model, mice with luciferase expressed in the liver were treated with PF6/luc-siRNA nanoparticles. By using doses up to 1 mg/kg, substantial luciferase knockdown was observed, which lasted for more than a week. Hydrodynamic injection is frequently considered the golden standard technique for achieving siRNA-mediated RNAi responses in liver (42). Intriguingly, RNAi responses with PF6/siRNA in liver were at least in line with that standard technique. These results are comparable to recently published results on the use of lipid nanoparticles (LNPs) for siRNA, targeting luciferase in liver of mice (43). Using LNPs with optimized composition (right amount of cationic liposomes, polyethylene glycol and cholesterol), the authors reported on significant RNAi responses for 10 days using doses of 3 mg/kg siRNA. The strong RNAi responses observed in liver could relate to the negative zeta-potential observed for PF6/siRNA in serum media since it has been previously reported that various lipid-based systems with negative surface charge efficiently target hepatic cells *in vivo* (44,45). Although stronger gene silencing in the liver has been reported at lower siRNA doses with cholesterol-functionalized and other lipid-based delivery systems, e.g. SNALP and lipidoids, these vehicles contain multiple components and require additional formulation procedures. The PF6-platform, however, works as a one-component system without any targeting motifs and it does not require cumbersome formulation procedures for being active. Also, we have utilized siRNAs composed of unmodified RNA, whereas in other studies different modifications have been exploited, which render siRNAs more stable against enzymatic degradation in the systemic circulation. Thus, there is room for improvement and by using stabilized siRNAs in combination with optimized formulations, the PF6/siRNA nanoparticles are likely to work at significantly lower doses.

Our results collectively demonstrate that PF6 has the desired *in vitro* properties of a promising transfection agent in that it promotes siRNA delivery to entire cell populations, is highly active in hard-to-transfect cells, is relatively tolerant to serum, and is essentially independent of cell confluence. Furthermore, PF6 displays very low toxicity according to microarray and proteomics analysis. Most importantly, the vector/siRNA complexes are suitable for systemic delivery without any observed toxicity, which implies that, in addition to having significant utility for RNAi screens *in vitro*, it has therapeutic potential.

SUPPLEMENTARY DATA

Supplementary Data are available at NAR Online.

ACKNOWLEDGEMENTS

We thank Mario Plaas for providing and culturing MEFs and ES-cells, Raivo Kolde for help with microarray analysis and Anna Forsby for providing the C17.2 neuronal stem cells, cloned by Evan Snyder. We thank Mark Behlke for help with HPRT1 siRNA sequence design and providing the Transductin™ reagent and Andres Merits for providing the EGFP-CHO cells. We thank Gösta Eggersten for analysis of clinical chemistry parameters and Per Lundin for proofreading the article.

FUNDING

Swedish Research Council (VR-NT); the Stockholm County Council (research grant ALF-projektmedel medicin); Swedish Governmental Agency for Innovation Systems (VINNOVA-SAMBIO2006); Centre of Biomembrane Research, Stockholm; Knut and Alice Wallenberg Foundation, Sweden; EU through the European Regional Development Fund through the Centre of Excellence in Chemical Biology and in Genomics, Estonia; targeted financing SF0180027s08; targeted financing from the Estonian Ministry of Education and Research (SF0180142s08 to A.M.); the Estonian Science Foundation (grant ETF7076); the EU FP7 grants ECOGENE (#205419, EBC); OPENGENE (#245536, UTARTU); the EU via the European Regional Development Fund grant to the Centre of Excellence in Genomics, the Estonian Biocentre; DoRa program of the European Social Fund; European Union FP6 grant EuroPharmacoGene (FP-2005-037283); Egyptian Ministry of higher Education (to E.M.Z.); Karolinska Institute Faculty funds for postgraduate students (to J.R.V.); Archimedes Foundation (to T.L. and I.M.); French AFM foundation (to F.S.H. and B.L.); ESF program 'Frontiers of Functional Genomics' grant (to J.H.); Swedish Society of Medical Research (SSMF to S.ELA). Funding for open access charge: Karolinska Institute, Department of Laboratory Medicine, SE-141 86 Huddinge, Sweden.

Conflict of interest statement. None declared.

REFERENCES

1. Fire,A., Xu,S., Montgomery,M.K., Kostas,S.A., Driver,S.E. and Mello,C.C. (1998) Potent and specific genetic interference by double-stranded RNA in Caenorhabditis elegans. *Nature*, **391**, 806–811.
2. Castanotto,D. and Rossi,J.J. (2009) The promises and pitfalls of RNA-interference-based therapeutics. *Nature*, **457**, 426–433.
3. de Fougerolles,A., Vornlocher,H.P., Maraganore,J. and Lieberman,J. (2007) Interfering with disease: a progress report on siRNA-based therapeutics. *Nat. Rev. Drug Discov.*, **6**, 443–453.
4. Whitehead,K.A., Langer,R. and Anderson,D.G. (2009) Knocking down barriers: advances in siRNA delivery. *Nat. Rev. Drug Discov.*, **8**, 129–138.

5. El Andaloussi,S., Holm,T. and Langel,Ü. (2005) Cell-penetrating peptides: mechanisms and applications. *Curr. Pharm Des.*, **11**, 3597–3611.
6. Meade,B.R. and Dowdy,S.F. (2008) Enhancing the cellular uptake of siRNA duplexes following noncovalent packaging with protein transduction domain peptides. *Adv. Drug Deliv. Rev.*, **60**, 530–536.
7. Tiemann,K. and Rossi,J.J. (2009) RNAi-based therapeutics-current status, challenges and prospects. *EMBO Mol. Med.*, **1**, 142–151.
8. Mae,M., Andaloussi,S.E., Lehto,T. and Langel,U. (2009) Chemically modified cell-penetrating peptides for the delivery of nucleic acids. *Expert Opin. Drug Deliv.*, **6**, 1195–1205.
9. Crombez,L., Morris,M.C., Dufort,S., Aldrian-Herrada,G., Nguyen,Q., Mc Master,G., Coll,J.L., Heitz,F. and Divita,G. (2009) Targeting cyclin B1 through peptide-based delivery of siRNA prevents tumour growth. *Nucleic Acids Res.*, **37**, 4559–4569.
10. Hatakeyama,H., Ito,E., Akita,H., Oishi,M., Nagasaki,Y., Futaki,S. and Harashima,H. (2009) A pH-sensitive fusogenic peptide facilitates endosomal escape and greatly enhances the gene silencing of siRNA-containing nanoparticles in vitro and in vivo. *J. Control Release*, **139**, 127–132.
11. Akita,H., Kogure,K., Moriguchi,R., Nakamura,Y., Higashi,T., Nakamura,T., Serada,S., Fujimoto,M., Naka,T., Futaki,S. *et al.* (2010) Nanoparticles for ex vivo siRNA delivery to dendritic cells for cancer vaccines: programmed endosomal escape and dissociation. *J. Control Release*, **143**, 311–317.
12. Eguchi,A., Meade,B.R., Chang,Y.C., Fredrickson,C.T., Willert,K., Puri,N. and Dowdy,S.F. (2009) Efficient siRNA delivery into primary cells by a peptide transduction domain-dsRNA binding domain fusion protein. *Nat. Biotechnol.*, **27**, 567–571.
13. Michiue,H., Eguchi,A., Scadeng,M. and Dowdy,S.F. (2009) Induction of in vivo synthetic lethal RNAi responses to treat glioblastoma. *Cancer Biol. Ther.*, **8**, 2304–2311.
14. Deshayes,S., Morris,M., Heitz,F. and Divita,G. (2008) Delivery of proteins and nucleic acids using a non-covalent peptide-based strategy. *Adv. Drug Deliv. Rev.*, **60**, 537–547.
15. Kumar,P., Wu,H., McBride,J.L., Jung,K.E., Kim,M.H., Davidson,B.L., Lee,S.K., Shankar,P. and Manjunath,N. (2007) Transvascular delivery of small interfering RNA to the central nervous system. *Nature*, **448**, 39–43.
16. Kumar,P., Ban,H.S., Kim,S.S., Wu,H., Pearson,T., Greiner,D.L., Laouar,A., Yao,J., Haridas,V., Habiro,K. *et al.* (2008) T cell-specific siRNA delivery suppresses HIV-1 infection in humanized mice. *Cell*, **134**, 577–586.
17. Lundberg,P., El-Andaloussi,S., Sütlü,T., Johansson,H. and Langel,Ü. (2007) Delivery of short interfering RNA using endosomolytic cell-penetrating peptides. *FASEB J.*, **21**, 2664–2671.
18. Cheng,J., Zeidan,R., Mishra,S., Liu,A., Pun,S.H., Kulkarni,R.P., Jensen,G.S., Bellocq,N.C. and Davis,M.E. (2006) Structure-function correlation of chloroquine and analogues as transgene expression enhancers in nonviral gene delivery. *J. Med. Chem.*, **49**, 6522–6531.
19. Mae,M., El Andaloussi,S., Lundin,P., Oskolkov,N., Johansson,H.J., Guterstam,P. and Langel,U. (2009) A stearylated CPP for delivery of splice correcting oligonucleotides using a non-covalent co-incubation strategy. *J. Control Release*, **134**, 221–227.
20. Pooga,M., Soomets,U., Hällbrink,M., Valkna,A., Saar,K., Rezaei,K., Kahl,U., Hao,J.X., Xu,X.J., Wiesenfeld-Hallin,Z. *et al.* (1998) Cell penetrating PNA constructs regulate galanin receptor levels and modify pain transmission in vivo. *Nat. Biotechnol.*, **16**, 857–861.
21. Eriksson,H., Lengqvist,J., Hedlund,J., Uhlen,K., Orre,L.M., Bjellqvist,B., Persson,B., Lehtio,J. and Jakobsson,P.J. (2008) Quantitative membrane proteomics applying narrow range peptide isoelectric focusing for studies of small cell lung cancer resistance mechanisms. *Proteomics*, **8**, 3008–3018.
22. Collingwood,M.A., Rose,S.D., Huang,L., Hillier,C., Amarzguioui,M., Wiiger,M.T., Soifer,H.S., Rossi,J.J. and Behlke,M.A. (2008) Chemical modification patterns compatible with high potency dicer-substrate small interfering RNAs. *Oligonucleotides*, **18**, 187–200.
23. Boyer,L.A., Lee,T.I., Cole,M.F., Johnstone,S.E., Levine,S.S., Zucker,J.P., Guenther,M.G., Kumar,R.M., Murray,H.L., Jenner,R.G. *et al.* (2005) Core transcriptional regulatory circuitry in human embryonic stem cells. *Cell*, **122**, 947–956.
24. de Godoy,L.M., Olsen,J.V., Cox,J., Nielsen,M.L., Hubner,N.C., Frohlich,F., Walther,T.C. and Mann,M. (2008) Comprehensive mass-spectrometry-based proteome quantification of haploid versus diploid yeast. *Nature*, **455**, 1251–1254.
25. Judge,A.D., Bola,G., Lee,A.C. and MacLachlan,I. (2006) Design of noninflammatory synthetic siRNA mediating potent gene silencing in vivo. *Mol. Ther.*, **13**, 494–505.
26. Liu,F., Song,Y. and Liu,D. (1999) Hydrodynamics-based transfection in animals by systemic administration of plasmid DNA. *Gene Ther.*, **6**, 1258–1266.
27. Bevan,A.P., Krook,A., Tikerpae,J., Seabright,P.J., Siddle,K. and Smith,G.D. (1997) Chloroquine extends the lifetime of the activated insulin receptor complex in endosomes. *J. Biol. Chem.*, **272**, 26833–26840.
28. Morris,M.C., Chaloin,L., Mery,J., Heitz,F. and Divita,G. (1999) A novel potent strategy for gene delivery using a single peptide vector as a carrier. *Nucleic Acids Res.*, **27**, 3510–3517.
29. Akinc,A., Zumbuehl,A., Goldberg,M., Leshchiner,E.S., Busini,V., Hossain,N., Bacallado,S.A., Nguyen,D.N., Fuller,J., Alvarez,R. *et al.* (2008) A combinatorial library of lipid-like materials for delivery of RNAi therapeutics. *Nat. Biotechnol.*, **26**, 561–569.
30. Zimmermann,T.S., Lee,A.C., Akinc,A., Bramlage,B., Bumcrot,D., Fedoruk,M.N., Harborth,J., Heyes,J.A., Jeffs,L.B., John,M. *et al.* (2006) RNAi-mediated gene silencing in non-human primates. *Nature*, **441**, 111–114.
31. Petros,R.A. and DeSimone,J.M. (2010) Strategies in the design of nanoparticles for therapeutic applications. *Nat. Rev. Drug Discov.*, **9**, 615–627.
32. Heitz,F., Morris,M.C. and Divita,G. (2009) Twenty years of cell-penetrating peptides: from molecular mechanisms to therapeutics. *Br. J. Pharmacol.*, **157**, 195–206.
33. Lundin,P., Johansson,H., Guterstam,P., Holm,T., Hansen,M., Langel,Ü. and Andaloussi,S.E.L. (2008) Distinct uptake routes of cell-penetrating peptide conjugates. *Bioconjug. Chem.*, **19**, 2535–2542.
34. El-Andaloussi,S., Jarver,P., Johansson,H.J. and Langel,Ü. (2007) Cargo-dependent cytotoxicity and delivery efficacy of cell-penetrating peptides: a comparative study. *Biochem. J.*, **407**, 285–292.
35. Kilk,K., Mahlapuu,R., Soomets,U. and Langel,Ü. (2009) Analysis of in vitro toxicity of five cell-penetrating peptides by metabolic profiling. *Toxicology*, **265**, 87–95.
36. Hornung,V., Guenthner-Biller,M., Bourquin,C., Ablasser,A., Schlee,M., Uematsu,S., Noronha,A., Manoharan,M., Akira,S., de Fougerolles,A. *et al.* (2005) Sequence-specific potent induction of IFN-alpha by short interfering RNA in plasmacytoid dendritic cells through TLR7. *Nat. Med.*, **11**, 263–270.
37. Judge,A. and MacLachlan,I. (2008) Overcoming the innate immune response to small interfering RNA. *Hum. Gene Ther.*, **19**, 111–124.
38. Kleinman,M.E., Yamada,K., Takeda,A., Chandrasekaran,V., Nozaki,M., Baffi,J.Z., Albuquerque,R.J., Yamasaki,S., Itaya,M., Pan,Y. *et al.* (2008) Sequence- and target-independent angiogenesis suppression by siRNA via TLR3. *Nature*, **452**, 591–597.
39. Robbins,M., Judge,A., Liang,L., McClintock,K., Yaworski,E. and MacLachlan,I. (2007) 2'-O-methyl-modified RNAs act as TLR7 antagonists. *Mol. Ther.*, **15**, 1663–1669.
40. Harris,T.J., Green,J.J., Fung,P.W., Langer,R., Anderson,D.G. and Bhatia,S.N. (2010) Tissue-specific gene delivery via nanoparticle coating. *Biomaterials*, **31**, 998–1006.
41. Moschos,S.A., Williams,A.E. and Lindsay,M.A. (2007) Cell-penetrating-peptide-mediated siRNA lung delivery. *Biochem. Soc. Trans.*, **35**, 807–810.
42. McCaffrey,A.P., Meuse,L., Pham,T.T., Conklin,D.S., Hannon,G.J. and Kay,M.A. (2002) RNA interference in adult mice. *Nature*, **418**, 38–39.

43. Tao,W., Davide,J.P., Cai,M., Zhang,G.J., South,V.J., Matter,A., Ng,B., Zhang,Y. and Sepp-Lorenzino,L. (2010) Noninvasive imaging of lipid nanoparticle-mediated systemic delivery of small-interfering RNA to the liver. *Mol. Ther.*, **18**, 1657–1666.
44. Bartsch,M., Weeke-Klimp,A.H., Meijer,D.K., Scherphof,G.L. and Kamps,J.A. (2002) Massive and selective delivery of lipid-coated cationic lipoplexes of oligonucleotides targeted in vivo to hepatic endothelial cells. *Pharm Res.*, **19**, 676–680.
45. Furumoto,K., Nagayama,S., Ogawara,K., Takakura,Y., Hashida,M., Higaki,K. and Kimura,T. (2004) Hepatic uptake of negatively charged particles in rats: possible involvement of serum proteins in recognition by scavenger receptor. *J. Control Release*, **97**, 133–141.